

Article

# Effect of the Titanium Isopropoxide:Acetylacetonone Molar Ratio on the Photocatalytic Activity of TiO<sub>2</sub> Thin Films

Jekaterina Spiridonova <sup>1,\*</sup>, Atanas Katerski <sup>1</sup>, Mati Danilson <sup>2</sup>, Marina Krichevskaya <sup>3,\*</sup>, Malle Krunk <sup>1</sup> and Ilona Oja Acik <sup>1,\*</sup>

<sup>1</sup> Laboratory of Thin Films Chemical Technologies, Department of Materials and Environmental Technology, Tallinn University of Technology, Ehitajate tee 5, 19086 Tallinn, Estonia; atanas.katerski@taltech.ee (A.K.); malle.krunk@taltech.ee (M.K.)

<sup>2</sup> Laboratory of Optoelectronic Materials Physics, Department of Materials and Environmental Technology, Tallinn University of Technology, Ehitajate tee 5, 19086 Tallinn, Estonia; mati.danilson@taltech.ee

<sup>3</sup> Laboratory of Environmental Technology, Department of Materials and Environmental Technology, Tallinn University of Technology, Ehitajate tee 5, 19086 Tallinn, Estonia

\* Correspondence: jekaterina.spiridonova@taltech.ee (J.S.); marina.kritsevskaja@taltech.ee (M.K.); ilona.oja@taltech.ee (I.O.A.); Tel.: +372-620-3369 (I.O.A.)

Academic Editors: Smagul Karazhanov, Ana Cremades and Cuong Ton-That

Received: 31 October 2019; Accepted: 25 November 2019; Published: 27 November 2019



**Abstract:** TiO<sub>2</sub> thin films with different titanium isopropoxide (TTIP):acetylacetonone (AcacH) molar ratios in solution were prepared by the chemical spray pyrolysis method. The TTIP:AcacH molar ratio in spray solution varied from 1:3 to 1:20. TiO<sub>2</sub> films were deposited onto the glass substrates at 350 °C and heat-treated at 500 °C. The morphology, structure, surface chemical composition, and photocatalytic activity of the obtained TiO<sub>2</sub> films were investigated. TiO<sub>2</sub> films showed a transparency of ca 80% in the visible spectral region and a band gap of ca 3.4 eV irrespective of the TTIP:AcacH molar ratio in the spray solution. TiO<sub>2</sub> films consist of the anatase crystalline phase with a mean crystallite size in the range of 30–40 nm. Self-cleaning properties of the films were estimated using the stearic acid (SA) test. A thin layer of 8.8-mM SA solution was spin-coated onto the TiO<sub>2</sub> film. The degradation rate of SA as a function of irradiation time was monitored by Fourier-transform infrared spectroscopy (FTIR). An increase in the TTIP:AcacH molar ratio from 1:4 to 1:8 resulted in a ten-fold increase in the photodegradation reaction rate constant (from 0.02 to the 0.2 min<sup>-1</sup>) under ultraviolet light and in a four-fold increase under visible light.

**Keywords:** TiO<sub>2</sub>; thin film; ultrasonic spray pyrolysis; acetylacetonone; photocatalysis; stearic acid

## 1. Introduction

The synthesis and optimization of TiO<sub>2</sub> thin films is a rapidly developing topic in the field of environmental engineering due to their great potential in pollution treatment and self-cleaning properties. Transparent glass has multiple applications. It is widely used in our homes (in windows, doors, and shower enclosures), in automobile windshields, in electronic device screens, and in construction materials for modern skyscrapers. Keeping the surface of the glass clean is not an easy task; due to its optical transparency, all the dirt particles, stains, and fingerprints which present on the surface are noticeable [1].

Today, more and more skyscrapers are built worldwide because they give us an opportunity to design a good deal of real estate using a relatively small ground area. However, skyscraper window cleaning is risky. According to the National Institute for Occupational Safety and Health (NIOSH) in

the United States there were 88 window cleaning accidents over a 15-year period; 70% of them ended in death [2]. Covering the surface of skyscrapers with a TiO<sub>2</sub> thin layer can substitute this risky job and save money (along with water and chemicals) on cleaning. TiO<sub>2</sub> has photocatalytic and hydrophilic properties when it is irradiated with light source that has an energy content equal to or higher than the band gap of the TiO<sub>2</sub>. One of the first commercialized applications of TiO<sub>2</sub> as a photocatalytic material was a self-cleaning glass for tunnel light covers in Japan. Tunnel lamps in Japan emit ultraviolet (UV) light of about 3 mW cm<sup>-2</sup>, which is enough to keep the glass cover surface clean of automobile exhaust when it is covered with the TiO<sub>2</sub> photocatalyst [3].

For commercial use, it is very important to find a cost-effective and efficient technology for thin film deposition. TiO<sub>2</sub> films have been prepared using a variety of deposition methods such as chemical vapor deposition [4], sputtering [5], hydrothermal [6], electrophoretic [7], sol-gel [8,9], and spray pyrolysis [10,11]. Among the above-mentioned methods, deposition of thin films with ultrasonic spray pyrolysis has the advantage of being a simple, inexpensive method that allows us to obtain transparent homogeneous films with high stability and quality. This method could be easily applied at the laboratory scale as well as in industry for film deposition on large surfaces [12,13]. Our research group is focused on gas-phase photocatalytic oxidation on TiO<sub>2</sub> thin films prepared by the spray pyrolysis technique. In our recent study, 350 °C was found as to be an optimal temperature for film deposition because this film has a greater number of surface defects [13].

Choosing a precursor solution for thin film preparation is the next essential step in the process of material synthesis. In solution preparation, mainly alkoxides are used as a titanium source, for example, titanium butoxide [12,14], titanium ethoxide [15], and titanium isopropoxide (TTIP) [8,13,16]. Since metal oxides are highly reactive with water, to stabilize the precursor solution and retard the hydrolysis rate, chemical additives are used. These can be acids (HCl) [17], bases (NaOH) [18], solvents (2-methoxyethanol) [9,19], or stabilizing agents (acetylacetone) [9,10,16]. The effects of organic additives such as benzoic acid [20], diethylene glycol [21], diethanolamine [22], humic acid [23], and glucose [24] on the properties of TiO<sub>2</sub> thin films and powder materials were studied. Byrne et al. (2016) have studied the effect of molar ratio TiO<sub>2</sub>:benzoic acid on the phase transformation and carbon incorporation onto the surface of photocatalyst and found that benzoic acid enhances rutile phase formation [20]. Park and co-authors (2009) studied the carbon incorporation into the lattice of TiO<sub>2</sub> photocatalyst prepared by sol-gel by changing the calcination temperature without the addition of external carbon source. Lattice carbon incorporation enhances the photocatalytic oxidation of 4-chlorophenol and iodide under visible light [25].

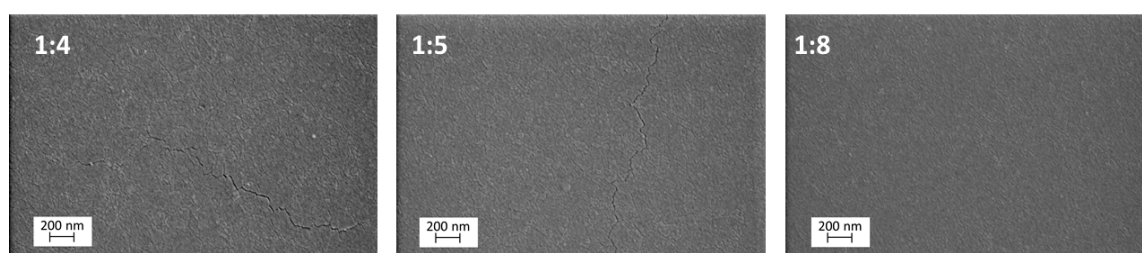
In the current study, modifications in the precursor solution were done to prepare a more active material. Titanium isopropoxide (TTIP) was used as a precursor and acetylacetone (AcacH) as a stabilizing agent. The reaction of TTIP with AcacH has been well studied in the literature. Acetylacetone behaves as a nucleophilic reactant and replaces the alkoxy group; thus, a new molecular precursor is formed [26]. This reaction has been studied using Fourier-transform infrared spectroscopy (FTIR) [16,27]. However, it is known that the TTIP:AcacH molar ratio 1:1 is not sufficient for complete complex formation; the complex is formed at the molar ratio of 1:2 and starting from the ratio 1:3 an excess of acetylacetone can be seen in the solution [16]. Few studies have focused on the effect of the TTIP:AcacH molar ratio on the structural properties [16] and photocatalytic activity of the films [28] and powders [29]. No comprehensive studies about addition of a high AcacH molar ratio into the precursor solution and its effects on the material and photocatalytic properties of the films were found in the scientific literature. The aim of this study was to determine the optimal TTIP:AcacH molar ratio in the precursor solution for the deposition of photocatalytically active TiO<sub>2</sub> thin films by the ultrasonic spray pyrolysis method. The morphological and structural properties, surface chemical composition, and photocatalytic activity of TiO<sub>2</sub> thin films with different TTIP:AcacH molar ratios (from 1:3 to 1:20) were investigated. The photocatalytic activity in the current study was tested by the stearic acid test under ultraviolet (UV-A) and visible light (VIS).

## 2. Results and Discussion

### 2.1. Surface Morphology

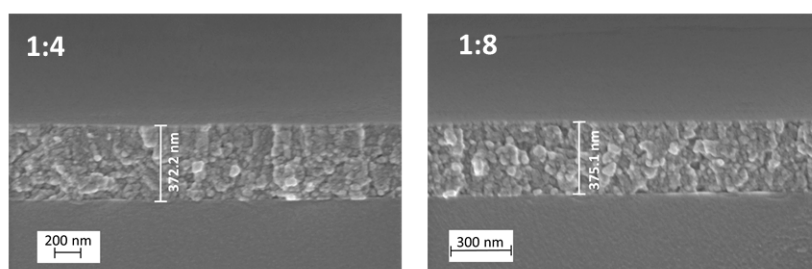
Scanning electron microscopy (SEM) images of the TiO<sub>2</sub> thin films with TTIP:AcacH molar ratios of 1:4, 1:5, and 1:8 are presented in Figure 1. An increase in the amount of acetylacetone in the precursor solution makes the surface of the thin film flatter, smoother, and more uniform. Kajitvichyanukul et al. (2005) have studied the effect of acetylacetone on the morphology of TiO<sub>2</sub> thin films prepared by sol-gel dip coating. They found that with the increase in acetylacetone, smooth films, like TiO<sub>2</sub> sheets, were obtained [30].

Figure 1 shows that the surfaces of 1:4 and 1:5 TTIP:AcacH thin films have cracks, while the 1:8 film surface is crack-free. Addition of acetylacetone to titanium isopropoxide makes the process of gel formation slower. Therefore, the precursor solution is more stable and homogeneous, promoting the synthesis of thin films with a higher quality and better adhesion [26].



**Figure 1.** Scanning electron microscopy (SEM) surface images of TiO<sub>2</sub> thin films deposited on borosilicate glass at titanium isopropoxide (TTIP):acetylacetone (AcacH) molar ratios of 1:4, 1:5, and 1:8.

The thicknesses of the samples with the molar ratios 1:4 and 1:8 were determined from their SEM cross-sectional images and were 370 and 375 nm, respectively (Figure 2). It was observed that the thickness of the TiO<sub>2</sub> thin films was not affected by the increase in the acetylacetone molar ratio in the starting solution.



**Figure 2.** Cross-sectional SEM images of TiO<sub>2</sub> thin films deposited on borosilicate glass at TTIP:AcacH molar ratios of 1:4 and 1:8.

### 2.2. Structural Properties

X-ray diffraction (XRD) analysis was performed to investigate crystallinity, phase composition, and the mean crystallite size of TiO<sub>2</sub> thin films. All of the obtained films consist only of the anatase phase regardless of the acetylacetone molar ratio in the precursor solution. Figure 3 reveals a diffractogram of TiO<sub>2</sub> films. The diffraction peaks at 2 theta of 25.3°, 37.0°, 37.8°, 38.6°, 48.1°, 53.9°, and 55° correspond to the reflection planes from (101), (103), (004), (112), (200), (105), and (211), respectively, of anatase TiO<sub>2</sub> [31]. No diffraction peaks belonging to the rutile or brookite phase were detected.

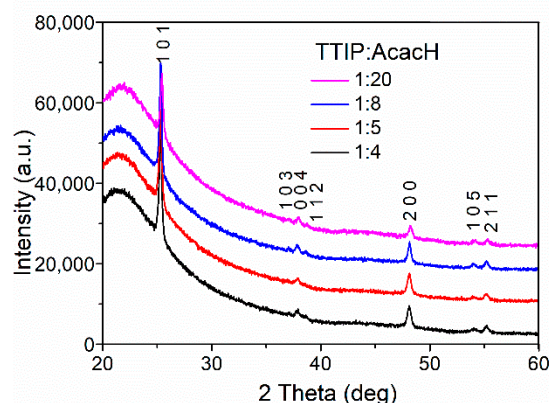


**Figure 3.** X-ray diffraction (XRD) patterns of TiO<sub>2</sub> thin films with different TTIP:AcacH molar ratios.

The mean crystallite size was calculated using the full width at half maximum (FWHM) of the most intense (101) peak of anatase phase by the Scherrer formula. The mean crystallite size of the films varies in the range of 30–40 nm. Slight changes in the values of crystallite size are not in correlation with the amount of acetylacetonate in the starting solution.

According to the literature, an increase of AcacH in the precursor solution affects the phase transformation process from anatase to rutile and enhances the crystallization process. The anatase to rutile phase transformation starts to occur at the annealing temperature about 800 °C when the precursor solution is not fully stabilized (in the case of a TTIP:AcacH molar ratio less than 1:3). Excess of AcacH in the starting solution lowers the transformation temperature by about 100 °C [16].

The results of this study demonstrate that an increase in the amount of the unchelated acetylacetonate in the precursor solution has no significant effect on the structural properties of TiO<sub>2</sub> thin films, since all the obtained films were annealed at the same temperature –500 °C.

### 2.3. Optical Properties

The optical transmittance spectra of TiO<sub>2</sub> thin films were measured in the wavelength range between 200 and 1200 nm (Figure 4). Obtained thin films are transparent in the visible light region. The transmittance is about 80% in the spectral region of 500–1200 nm for all obtained films irrespective of the TTIP:AcacH molar ratio in the spray solution.

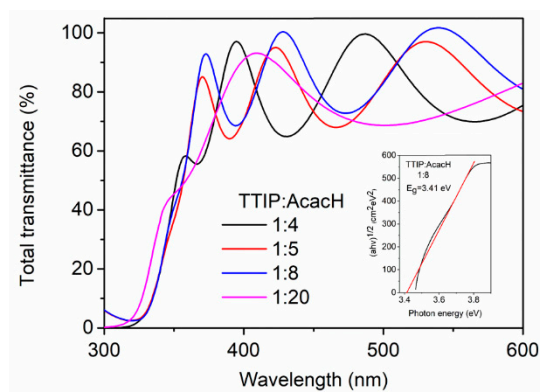


**Figure 4.** Total transmittance spectra for TiO<sub>2</sub> thin films deposited at different TTIP:AcacH molar ratios. The inset shows the band gap value of the sample deposited at the TTIP:AcacH molar ratio of 1:8.

Using maxima or/and minima of interference fringes of the optical spectrum, it is possible to investigate the thickness of the film by the so called Swanepoel's method. Thickness ( $d$ ) can be found by the following equation:

$$d = \frac{\lambda_1 \lambda_2}{2(\lambda_1 n_2 - \lambda_2 n_1)}, \quad (1)$$

where  $n_1$  and  $n_2$  are reflective indexes at two adjacent maxima/minima, and  $\lambda_1 \lambda_2$  is the wavelength of the maxima/minima [32].

The thickness calculated by Swanepoel's method corresponds to the thickness that was determined by SEM cross-sectional images (Figure 2, Section 2.1.) and is about 400 nm for all samples (Table 1), except for the sample with the TTIP:AcacH molar ratio of 1:20. This sample is about 100 nm thinner. This could be explained by a rise in the amount of free AcacH in precursor solution that increased the viscosity of the spray solution. Viscosity affects the transportation of aerosol produced by an ultrasonic generator. The aerosol flow rate decreases with the increase in the viscosity value. As a result, the growth of the thin film occurs more slowly [33].

The band gap was found using the Tauc plot. Since TiO<sub>2</sub> has an indirect band gap, a plot of the  $\sqrt{\alpha E}$  function of photon energy,  $E = h\nu$ , was used [34]. Table 1 shows the band gaps of the obtained TiO<sub>2</sub> thin films, which are about 3.4 eV.

**Table 1.** Optical properties of TiO<sub>2</sub> thin films with different TTIP:AcacH ratios.

TTIP:AcacH Molar Ratio	Thickness, nm	Band Gap, eV
1:3	380	3.3
1:4	370	3.4
1:5	370	3.4
1:6	410	3.4
1:7	370	3.4
1:8	375	3.4
1:10	370	3.4
1:12	390	3.4
1:20	280	3.5

Overall, it was found that the optical properties of the TiO<sub>2</sub> films are not significantly affected by the acetylacetone amount in the precursor solution.

#### 2.4. Chemical Composition and Wettability

X-ray photoelectron spectroscopy (XPS) study was performed to investigate the chemical composition and bonding structure of the obtained TiO<sub>2</sub> thin films. The XPS spectra of TiO<sub>2</sub> thin films after UV-A pre-treatment for O<sub>1s</sub> and C<sub>1s</sub> core levels are represented in Figure 5.

O<sub>1s</sub> core level spectra consist of three peaks (Figure 5). The highest peak at the binding energy (BE) value 530.0 eV corresponds to the Ti-O bond. The peak at the BE value 531.0 eV indicates the O<sup>2-</sup> ions in oxygen-deficient regions within the matrix of TiO<sub>2</sub> [35], which could be associated with oxygen vacancies (V<sub>o</sub>), and the peak at the BE value 532.0 eV corresponds to hydroxyl groups adsorbed on the surface [36,37].

The carbon region consists of five singlets with maxima located at 285.0 eV, 285.9 eV, 286.9 eV, 288.5 eV, and 289.5 eV. The highest peak located at 285.0 eV originates from the C=C bond. The peak with the BE maxima at 285.9 eV corresponds to surface hydrocarbons. These forms of non-oxygenated carbons belong to contaminants adsorbed on the TiO<sub>2</sub> surface. Some studies propose that this carbon may exist in the grain boundaries of TiO<sub>2</sub> and it therefore acts as a photosensitizer [37,38]. Peaks with the BE values 286.9 eV and 288.5 eV represent the oxygen-bound species C-O and Ti-O-C bonds, respectively [39]. These peaks confirm the incorporation of carbon into the lattice in the place of the Ti atoms, i.e., interstitial carbon doping takes place [38].

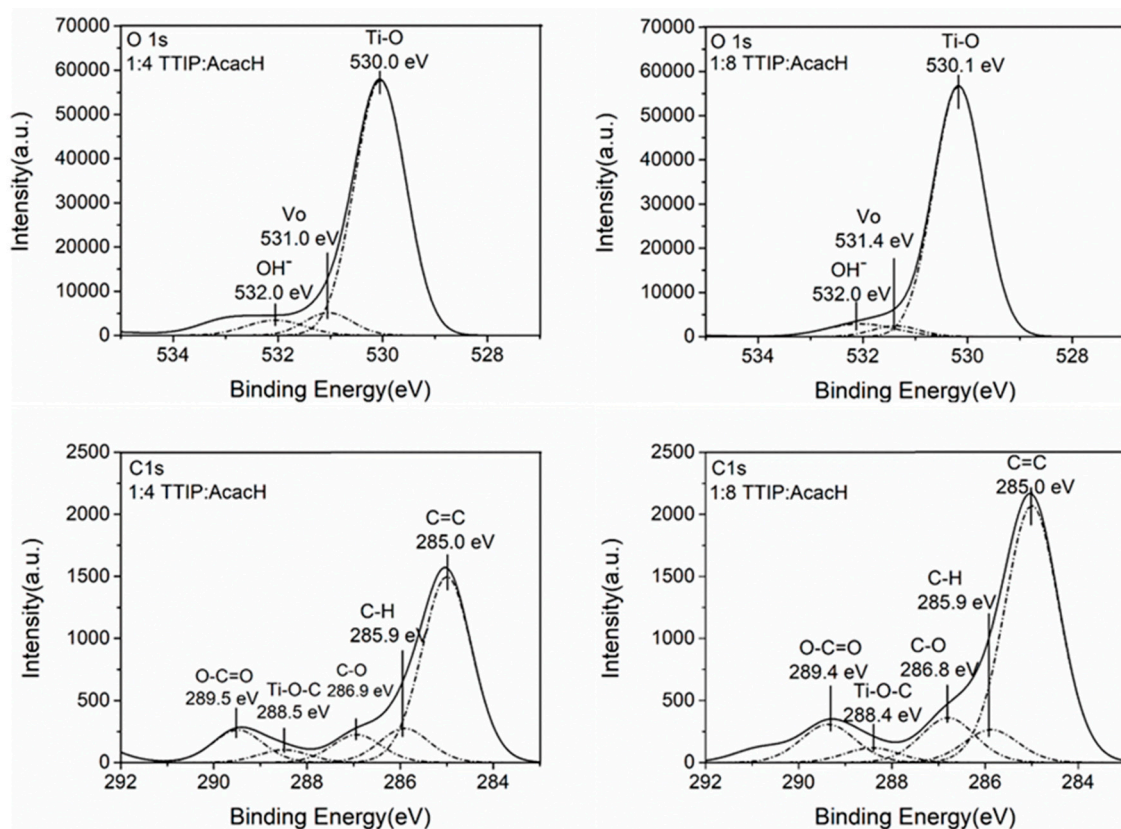


**Figure 5.** X-ray photoelectron spectroscopy (XPS) spectra of  $C_{1s}$  and  $O_{1s}$  core levels for 1:4 and 1:8 TTIP:AcacH molar ratios for  $TiO_2$  thin films after ultraviolet (UV-A) pre-treatment.

The integrated areas of the peaks were used to calculate atomic concentrations of the chemical components. The atomic ratios of the components  $(OH^-)/(Ti-O)$ ,  $(Vo)/(Ti-O)$ ,  $(C-O)/(C=O)$  and  $(C=C)/(C=O)$  ratios are presented in Table 2. There is no significant difference in the amount of oxygen vacancies and hydroxyl groups with the increase in AcacH, since the deposition parameters were the same. In their study, Dündar et al. (2019) showed that oxygen defects and the hydroxyl group amount on the surface depend on the temperature of the deposition [13].

**Table 2.** XPS data of the  $TiO_2$  thin films after UV-A pre-treatment.

TTIP:AcacH Molar Ratio	$(Vo)/(Ti-O)$ (at%/at%)	$(OH^-)/(Ti-O)$ (at%/at%)	$(C-O)/(C-H)$ (at%/at%)	$(Ti-O-C)/(C-H)$ (at%/at%)	$(C=C)/(C-H)$ (at%/at%)
1:4	0.08	0.07	0.8	0.38	5.43
1:8	0.06	0.07	1.35	0.44	7.80

XPS results showed that films with the higher AcacH molar ratio of 1:8 contained more adsorbed carbon on the surface of the film than films with TTIP:AcacH molar ratio of 1:4. It indicates that the surface of the 1:8 film could be more active since during the photocatalytic experiments, the oxidation of surface contaminant carbon takes place that leads to the increased number of active sites on the surface of the thin film [40]. The amount of C-O and Ti-O-C at the molar ratio 1:8 is also higher, which means that carbon from the unchelated acetylacetonate is transported to the  $TiO_2$  lattice during the decomposition of organic matter. It is reported in the literature that carbon doping enhances photocatalytic activity since it results in localized states occupied in the band gap [41,42]. One carbon atom incorporation into the  $TiO_2$  lattice in an interstitial position generates three strong covalent C-O bonds. These bonds in turn, create three bonding C-O states below the bottom of the  $O_{2p}$  valence band. Corresponding antibonding C-O states with high energy lie in the conduction band. The carbon

impurity in the interstitial position leads to the excess of electrons. Excess electrons moves from C-O state to the  $Ti_{3d}$ , not to corresponding C-O antibonding states, which creates two new occupied states in the band gap,  $Ti_{3d}$  and  $C_{2p}$ , below the bottom of the conduction band [43].

The wettability of the  $TiO_2$  film surface was measured for as-deposited films after thermal treatment, one-month aged films, and for aged films after 15 min of UV-A pre-treatment. The average water contact angle (CA) values are shown in Table 3. There is no difference in wettability for as prepared samples with an increase of AcacH in precursor solution; both surfaces are hydrophilic with a CA of about  $20^\circ$ . After one month of storage in the plastic box hydrophilic properties of the films decreased while the sample with a lower AcacH molar ratio (1:4) had significantly higher CA. Contact angles increased to  $55^\circ$  and  $30^\circ$  for TTIP:AcacH molar ratios of 1:4 and 1:8, respectively. This means that the increase of acetylacetonate in the precursor solution helps to keep the surface of the films photoinduced for a longer period of time, i.e., adsorption of water and contaminants from the ambient air on the surface of the  $TiO_2$  film with a TTIP:AcacH molar ratio of 1:8 occurs more slowly than at a ratio of 1:4. [44–46]. However, after 15 min of UV-A pre-treatment, all samples became super-hydrophilic, with CA less than  $5^\circ$ .

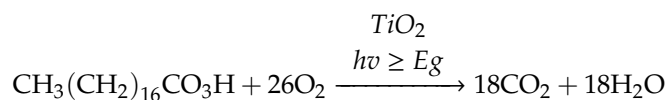
**Table 3.** Water contact angle values of as-deposited, one-month aged, and UV-A pre-treated films.

TTIP:AcacH Molar Ratio	Contact Angle $^\circ$		
	As-Deposited	One-month Aged	UV-A 15 min
1:4	20	55	4
1:8	20	30	0

During the UV-A pre-treatment water molecules desorb from  $TiO_2$  surface and hydroxyl groups are formed, leading to a better wetting of the surface [46]. This is in accordance with the XPS results showing that after UV-A pre-treatment, the number of hydroxyl groups on the  $TiO_2$  surface is the same for TTIP:AcacH molar ratios of 1:4 and 1:8 (Table 2). During the UV-A pre-treatment, besides hydroxyl groups, peroxy species ( $H_2O_2$ ) are formed on the surface of the photocatalyst, which increases the photocatalytic activity of the material [47,48]. Organic substances on the surface of  $TiO_2$  act as electron donors and enhance the production of  $H_2O_2$  [47].

### 2.5. Photocatalytic Activity. Stearic Acid Test

The stearic acid (SA) test is a method for assessing the activity of self-cleaning photocatalyst films. The essence of this method is a deposition of a thin layer of SA onto the film of photocatalytic material and monitoring of the the destruction of SA as a function of irradiation time. The overall reaction can be summarized as follows:



The most commonly employed method of monitoring photodegradation of stearic acid is via the disappearance of the SA film using infrared absorption spectroscopy. SA absorbs strongly in the region  $2700\text{--}3000\text{ cm}^{-1}$ , with peaks at  $2958\text{ cm}^{-1}$ ,  $2923\text{ cm}^{-1}$ , and  $2853\text{ cm}^{-1}$  due to asymmetric in-plane C-H stretching in the  $CH_3$  group and asymmetric and symmetric C-H stretching in the  $CH_2$  groups, respectively (Figure 6a) [49–51].

A stearic acid layer was deposited after the  $TiO_2$  film was pre-treated under UV-A to make the surface of the film photo-induced and super-hydrophilic. The decrease in stearic acid bond intensity was observed by FTIR measurements as a function of irradiation time. FTIR spectra were measured before the UV-A/VIS irradiation and every 15 min during an hour. The integrated area of the band was used to measure the degradation of stearic acid. It has been observed by several authors [52] that the surface structural and wettability properties of the films affect the growth of SA layer on the

surface of a photocatalytic material. Smirnova et al. (2015) detected a serious difference in the SA peaks intensities for TiO<sub>2</sub> thin films annealed at different temperatures [52]. In this study, films have similar structural and wettability properties (Sections 2.2 and 2.4); therefore, the initial integrated area of SA is almost the same.

Degradation of SA is known to follow first-order kinetics, i.e., the integrated band area (A) depends on time as follows:

$$A(t) = A_0 e^{-kt}, \quad (2)$$

where  $k$  is photodegradation rate constant. The photodegradation rate constant is the slope value of the linear fit of the plot  $\ln(A/A_0)$  versus  $t$  [53]. The degradation of stearic acid by TiO<sub>2</sub> at the TTIP:AcacH molar ratio 1:4 and determination of the photodegradation rate constant are presented in Figure 6.

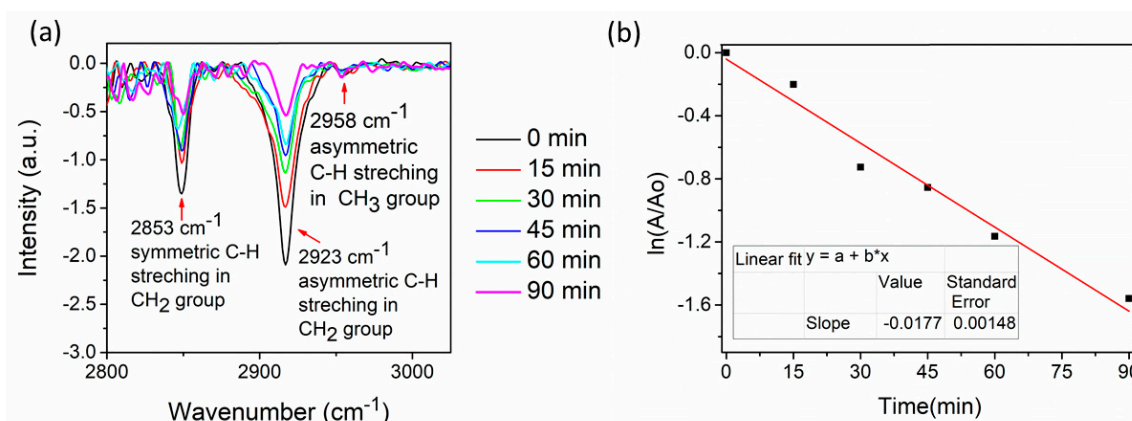


**Figure 6.** Fourier-transform infrared spectroscopy (FTIR) spectra of stearic acid on the surface of TiO<sub>2</sub> at the TTIP:AcacH molar ratio of 1:4 (a) and determination of the photodegradation rate constant ( $k$ ) at the molar ratio of 1:4 (b).

The degradation of the stearic acid layer as a function of UV-A irradiation time and the photodegradation rate constants ( $k$ ) at different TTIP:AcacH molar ratios under UV-A and VIS light for obtained TiO<sub>2</sub> thin films are illustrated in Figure 7.

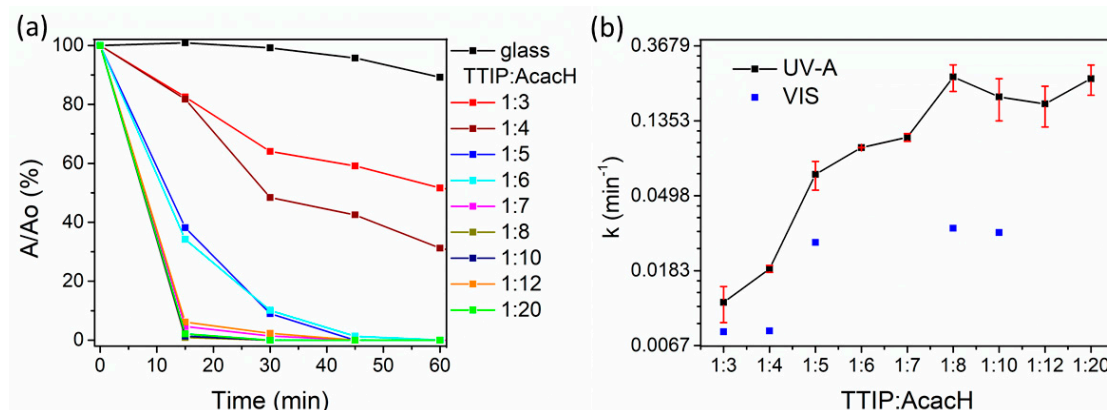


**Figure 7.** The degradation of stearic acid as a function of ultraviolet (UV-A) irradiation time (a) and photodegradation rate constants ( $k$ ) under UV-A and visible (VIS) light (b) for TiO<sub>2</sub> thin films at different TTIP:AcacH molar ratios.

Figure 7 shows that the increase in acetylacetone in the precursor solution results in a rapid increase in the photodegradation rate of SA. As can be seen in Figure 7a, for the TTIP:AcacH molar ratios of 1:3 and 1:4, 60 min of UV-A irradiation were not sufficient for complete degradation of the 8.8-mM SA layer; the degradation values were 48% and 69%, respectively. For the molar ratios of

1:5 and 1:6, the degradation was about 90% after 30 min, while at the higher ratios 1:7–1:20, almost complete degradation was achieved after 15 min of UV-A irradiation.

Pore et al. (2006) achieved complete degradation of the 8.8-mM SA layer degradation for atomic layer-deposited TiO<sub>2</sub> thin films modified with H<sub>2</sub>S after 60 min of UV-A irradiation, while an unmodified TiO<sub>2</sub> film was capable of degrading only half of SA at the same time of irradiation [51]. The optimal TTIP:AcacH molar ratio found was 1:8 at the reaction rate constant value 0.2427 min<sup>-1</sup>. As Figure 7b shows, after the molar ratio 1:8, the precursor solution is saturated with AcacH. The plateau is formed and no more increase in the photodegradation rate occurs.

According to many authors, carbon doping enhances photocatalytic activity under visible light [25,54–59]. Therefore, some of the films were tested for the ability to degrade the stearic acid layer under VIS light (Figure 7b). Photodegradation rate constants under VIS light are on average five times lower than under UV-A light. However, the trend in the increase of *k* value with the increase in amount of AcacH is similar to the case of UV-A. Films were not capable of full mineralization of the SA layer after 60 min of VIS irradiation. However, the conversion of SA was about 90% for samples at 1:8 and 1:10. Ratova et al. (2018) found that interstitial carbon doping enhances the photocatalytic activity of the reactively co-sputtered TiO<sub>2</sub> films under UV and VIS light [55]. However, the red shift of the band gap to the visible spectra was not observed in the present study (Table 1). The enhanced photocatalytic activity of the films under UV-A caused by an increase of AcacH can be due to the formation of C-O bonds, which could form new occupied states in the band gap (Section 2.4) [43].

### 3. Materials and Methods

#### 3.1. TiO<sub>2</sub> Thin Film Synthesis

TiO<sub>2</sub> thin films were deposited onto borosilicate glass substrates by the ultrasonic spray pyrolysis technique. Titanium (IV) isopropoxide (TTIP) was used as a titanium source, acetylacetone (AcacH) as a stabilizing agent, and ethanol as a solvent. All the deposition parameters were kept constant except the amount of acetylacetone in the precursor solution. The molar ratio of TTIP:AcacH in the precursor solution varied from 1:3 to 1:20. The TTIP concentration in the precursor solution was 0.2 M. To prepare the precursor solutions different amounts of acetylacetone were added to the 3.5 mL TTIP and after some minutes of mixing, the solution was adjusted to the 60 mL by ethanol. Prepared solutions were stirred for one hour. Aerosol produced by an ultrasonic generator was transported by compressed air with a flow rate of 5 L/min. The deposition temperature was set up to 350 °C. As-deposited samples were annealed at 500 °C for 1 h in air.

#### 3.2. Characterization of Films

Scanning electron microscope (SEM, Carl Zeiss, Jena, Germany) was used to investigate the surface morphology of the samples and cross-section images were used to determine the thickness of the films. X-ray diffraction (XRD) was used to study structural properties of the obtained TiO<sub>2</sub> thin films. The XRD diffractograms were obtained from the Rigaku Ultima IV diffractometer (Tokyo, Japan) with Cu K $\alpha$  radiation of  $\lambda = 1.5406 \text{ \AA}$ , 40 kV, at 40 mA, using a silicon strip detector. The measurements were performed in 2 theta configurations with the scan range 20–60°, with a scanning speed rate of 5° min<sup>-1</sup> and a step of 0.02°. The mean crystallite size was calculated using the Scherrer formula from the full width at half maximum (FWHM) of the most intense peak (101) reflection of TiO<sub>2</sub> anatase phase. Optical properties were measured with Jasco V-670 UV-VIS-NIR spectrophotometer (Tokyo, Japan) equipped with an integrating sphere in the spectral range 250–1500 nm. X-ray photoelectron spectroscopy (XPS) with use of a Kratos Analytical AXIS ULTRA DLD spectrometer (Manchester, England) in conjunction with a 165-mm hemispherical electron energy analyzer (Kratos Analytical, Manchester, England) and delay-line detector (Kratos Analytical, Manchester, England) was used to investigate the chemical composition of the surface of TiO<sub>2</sub> thin films. The analysis was carried out with monochromatic Al K $\alpha$  X-rays (1486.6 eV) operating at 15 kV and 150 W. All XPS spectra were

recorded using an aperture slot of 300–700 nm and pass energy of 20 eV. Binding energy (BE) values were calculated based on the C1s core level peak at 285.0 eV. Wettability of the films was studied with water contact angle (CA) measurements.

### 3.3. Evaluation of Photocatalytic Activity

Photocatalytic activity of the thin films was studied using a stearic acid (SA) test. A thin layer of 8.8-mM SA solution was deposited onto the TiO<sub>2</sub> thin film by the spin coating technique. For this, 100 µL of SA solution in methanol was dropped onto the center of the film (dimensions of the sample ≈ 2 × 2 cm). The rotation speed was 1000 rpm and the rotation time was 30 s. After the deposition, samples with stearic acid layer were dried at 80 °C in air for 10 min. The degradation of SA as a function of UV-A or VIS irradiation time was monitored by Fourier-transform infrared spectroscopy (FTIR, PerkinElmer, Beaconsfield, England) in the wavenumber region 3200–2500 cm<sup>-1</sup> in a transmission mode [46,47]. The instrument parameters for the measurements were as follows: wavenumber region 3200–2500 cm<sup>-1</sup>, number of scans 32, resolution 4 cm<sup>-1</sup>. The UV Philips Actinic BL 15 W (Philips, Poland), irradiance 3.5 mW cm<sup>-2</sup> with reflector (integrated in the range of 180–400 nm, with maximum emission at 365 nm, UV-B/UV-A ratio < 0.2%) or the VIS Philips TL-D 15 W (Philips, Poland), irradiance 3.3 mW cm<sup>-2</sup> with reflector lamps (integrated in the range of 180–700 nm, UV/UV-VIS ratio < 5%) were used as an irradiation source. The sample of the TiO<sub>2</sub> thin film without a stearic acid layer on it was used as a background during all the measurements. The integrated area of the bands was used to measure the degradation of stearic acid.

## 4. Conclusions

TiO<sub>2</sub> thin films with TTIP:AcacH molar ratios from 1:3 to 1:20 were deposited on a borosilicate glass substrate. The quantity of acetylacetone in the precursor solution had no significant effect on the optical and structural properties of the TiO<sub>2</sub> thin films. Films consisted of the anatase phase, with a band gap in the range of 3.3–3.5 eV and thickness in the range of 280–410 nm. However, the morphological study of the TiO<sub>2</sub> films showed that an increase in AcacH quantity in the precursor solution made the surface of the thin film more uniform.

Photocatalytic activity of the TiO<sub>2</sub> thin films with different TTIP:AcacH molar ratios was studied by the stearic acid test under UV-A and VIS light. It was found that with the increase in AcacH in the precursor solution, the photodegradation rate of stearic acid increased rapidly under both irradiations. However, as expected, the photocatalytic activity of the films was much higher under UV-A. The film with TTIP:AcacH molar ratio 1:8 had the highest activity in SA degradation under UV-A with the reaction rate constant  $k = 0.2427 \text{ min}^{-1}$ , which is 10 times higher compared to the molar ratio 1:4. The film with the molar ratio of 1:8 also showed maximum activity under VIS with  $k = 0.0323 \text{ min}^{-1}$ , which is four times higher than for the molar ratio 1:4. The optimal molar ratio of TTIP:AcacH 1:8 for ultrasonically sprayed TiO<sub>2</sub> thin films, which was found in this study, could be also applied for other chemical solution deposition techniques to produce photocatalytically efficient films.

The photodegradation rate of SA is enhanced with an increase in the AcacH amount in the precursor solution due to changes in the morphological and wettability properties and due to the incorporation of carbon into the TiO<sub>2</sub> lattice. XPS results showed that the film with a higher AcacH molar ratio contains more adsorbed carbon (BE = 285 eV) on the surface of the film and more carbon incorporated into the lattice of TiO<sub>2</sub>, which presumably improves the photocatalytic activity of the films.

**Author Contributions:** J.S. performed the deposition and characterization (XRD, optical properties, wettability, stearic acid test) of the films, participated in data collection and formal analysis, and participated in writing of the original draft; A.K. participated in material synthesis, data curation, and software; M.D. carried out the XPS measurements and XPS data formal analysis; M.K. (Marina Krichevskaya) participated in writing of the manuscript and formal analysis; M.K. (Malle Krunk) participated in formal analysis, project administration, and acquisition; I.O.A. supervised the study and participated in formal analysis, writing of manuscript, and project administration. All authors participated in manuscript review and editing and gave final approval for publication.

**Funding:** This research was funded by the Estonian Ministry of Education and Research, Estonian Research Council projects IUT19-4 and IUT19-28, and the Estonian Centre of Excellence project TK141. This work has been partially supported by the ASTRA TUT Institutional Development Programme for the 2016–2022 Graduate School of Functional Materials and Technologies (2014–2020.4.01.16-0032).

**Acknowledgments:** The authors acknowledge Olga Volobujeva for SEM measurements.

**Conflicts of Interest:** The authors declare no conflict of interest.

## References

1. Adachi, T.; Latthe, S.S.; Gosavi, S.W.; Roy, N.; Suzuki, N.; Ikari, H.; Kato, K.; Katsumata, K.; Nakata, K.; Furudate, M.; et al. Photocatalytic, superhydrophilic, self-cleaning TiO<sub>2</sub> coating on cheap, lightweight, flexible polycarbonate substrates. *Appl. Surf. Sci.* **2018**, *458*, 917–923. [CrossRef]
2. Falling is Every Window Cleaner's Nightmare. When His Scaffolding Broke Five Stories up, Jim Willingham Had to Think Fast. Available online: <https://consumer.healthday.com/encyclopedia/work-and-health-41/occupational-health-news-507/window-washers-646930.html> (accessed on 2 October 2019).
3. Hashimite, K.; Irie, H.; Fujishima, A. TiO<sub>2</sub> Photocatalysis: A Historical Overview and Future Prospects. *Jpn. J. Appl. Phys.* **2005**, *44*, 8269–8285. [CrossRef]
4. Mauchauffé, R.; Kang, S.; Kim, J.; Kim, J.H.; Moon, S.Y. Spectroscopic study of an atmospheric pressure plasma generated for the deposition of titanium dioxide thin films. *Curr. Appl. Phys.* **2019**, *19*, 1296–1304. [CrossRef]
5. Wei, B.; Xue, J.L.; Cao, H.T.; Li, H.G.; Wen, F.; Pei, Y.T. Effects of annealing on the composition, structure and photocatalytic properties of C-doped titania films deposited by reactive magnetron sputtering using CO<sub>2</sub> as carbon source. *Surf. Rev. Lett.* **2019**, *26*. [CrossRef]
6. Rahman, K.H.; Kumar, A.K. Effect of precursor concentration of microstructured titanium-di-oxide (TiO<sub>2</sub>) thin films and their photocatalytic activity. *Mater. Res. Express* **2019**, *6*. [CrossRef]
7. Sayahi, H.; Mohsenzadeh, F.; Hamadani, M. Cost-effective fabrication of perdurable electrodeposited TiO<sub>2</sub> nano-layers on stainless steel electrodes applicable to photocatalytic degradation of methylene blue. *Res. Chem. Intermed.* **2019**, *45*, 4275–4286. [CrossRef]
8. Tariq, M.K.; Riaz, A.; Khan, R.; Wajid, A.; Haq, H.; Javed, S.; Akram, M.A.; Islam, M. Comparative study of Ag, Sn or Zn doped TiO<sub>2</sub> thin films for photocatalytic degradation of methylene blue and methyl orange. *Mater. Res. Express* **2019**, *6*. [CrossRef]
9. Es-Souni, M.; Oja, I.; Krunk, M. Chemical solution deposition of thin TiO<sub>2</sub>-anatase films for dielectric applications. *J. Mater. Sci.-Mater. El.* **2014**, *15*, 341–344. [CrossRef]
10. Acik, I.O.; Katerski, A.; Mere, A.; Aarik, J.; Aidla, A.; Dedova, T.; Krunk, M. Nanostructured solar cell by spray pyrolysis: Effect of titania barrier layer on the cell performance. *Thin Solid Film.* **2009**, *517*, 2443–2447. [CrossRef]
11. Cergel, M.S.; Menir, E.; Atay, F. The effect of the structural, optical, and surface properties of anatase - TiO<sub>2</sub> film on photocatalytic degradation of methylene blue organic contaminant. *Ionic* **2019**, *25*, 4481–4492. [CrossRef]
12. Rasoulnezhad, H.; Hosseinzadeh, G.; Ghasemian, N.; Hosseinzadeh, R.; Keihan, A.H. Transparent nanostructured Fe-doped TiO<sub>2</sub> thin films prepared by ultrasonic assisted spray pyrolysis technique. *Mater. Res. Express* **2018**, *5*. [CrossRef]
13. Dündar, I.; Krichevskaya, M.; Katerski, A.; Oja-Acik, I. TiO<sub>2</sub> thin films by ultrasonic spray pyrolysis as photocatalytic material for air purification. *R. Soc. Open Sci.* **2019**, *6*, 1–12. [CrossRef]
14. Muniz-Serrato, O.; Serrato-Rodriguez, J. Formation of flow coated high catalytic activity thin films from the low temperature sol-gel titanium butoxide precursor. *J. Ceram. Res.* **2018**, *19*, 306–310.
15. With, P.C.; Helmstedt, U.; Naumov, S.; Sobottka, A.; Prager, A.; Decker, U.; Heller, R.; Abel, B.; Prager, L. Low-Temperature Photochemical Conversion of Organometallic Precursor Layers to Titanium(IV) Oxide Thin Films. *Chem. Mater.* **2016**, *28*, 7715–7724. [CrossRef]
16. Juma, A.O.; Oja Acik, I.; Mikli, V.; Mere, A.; Krunk, M. Effect of solution composition on anatase to rutile transformation of sprayed TiO<sub>2</sub> thin films. *Thin Solid Films* **2015**, *594*, 287–292. [CrossRef]
17. Lourduraj, S.; Williams, V. Effect of molarity on sol-gel routed nano TiO<sub>2</sub> thin films. *J. Adv. Dielectr.* **2017**, *7*, 7. [CrossRef]

18. Vernardou, D.; Vlachou, K.; Spanakis, E.; Stratakis, E.; Katsarakis, N.; Kymakis, E.; Koudoumas, E. Influence of solution chemistry on the properties of hydrothermally grown TiO<sub>2</sub> for advanced applications. *Catal. Today* **2009**, *144*, 172–176. [[CrossRef](#)]
19. Yamazaki, S.; Uchiyama, H.; Kozuka, H. Additive-free alkoxide–water–alcohol solutions as precursors for crystalline titania thin films. *J. Sol.-Gel Sci. Techn.* **2018**, *87*, 537–543. [[CrossRef](#)]
20. Byrne, C.; Fagan, R.; Hinder, S.; McCormack, D.E.; Pillai, S.C. New approach of modifying the anatase to rutile transition temperature in TiO<sub>2</sub> photocatalysts. *R. Soc. Chem.* **2016**, *6*, 95232–95238. [[CrossRef](#)]
21. Kajitvichyanukul, P.; Amornchat, P. Effects of diethylene glycol on TiO<sub>2</sub> thin film properties prepared by sol–gel process. *Sci. Techn. Adv. Mater.* **2005**, *6*, 344–347. [[CrossRef](#)]
22. Arjan, W.A.; Hector, A.L.; Levason, W. Speciation in diethanolamine-moderated TiO<sub>2</sub> precursor sols and their use in film formation. *J. Sol.-Gel Sci. Technol.* **2016**, *79*, 22. [[CrossRef](#)]
23. Wu, W.; Shan, G.; Xiang, Q.; Zhang, Y.; Yi, S.; Zhu, L. Effects of humic acids with different polarities on the photocatalytic activity of nano-TiO<sub>2</sub> at environment relevant concentration. *Water Res.* **2017**, *122*, 78–85. [[CrossRef](#)]
24. Maletic, M.; Vukcevic, M.; Kalijadis, A.; Jankovic–Castvan, I.; Dapcevic, A.; Lausevic, Z.; Lausevic, M. Hydrothermal synthesis of TiO<sub>2</sub>/carbon composites and their application for removal of organic pollutants. (in press)
25. Park, Y.; Kim, W.; Park, H.; Tachikawa, T.; Majima, T.; Choi, W. Carbon-doped TiO<sub>2</sub> photocatalyst synthesized without using an external carbon precursor and the visible light activity. *Appl. Catal. B-Environ.* **2009**, *91*, 355–361. [[CrossRef](#)]
26. Moon, J.; Li, T.; Randall, C.A.; Adair, J.H. Low temperature synthesis of lead titanate by a hydrothermal method. *J. Mater. Res.* **1997**, *12*, 189–197. [[CrossRef](#)]
27. Leautic, A.; Babonneau, F.; Livage, J. Structural Investigation of the Hydrolysis–Condensation Process of Titanium Alkoxides Ti(OR)<sub>4</sub> (OR = OPr<sub>1</sub>, OEt) Modified by Acetylacetone. 1. Study of the Alkoxide Modification. *Chem. Mater.* **1989**, *1*, 240–247. [[CrossRef](#)]
28. Kaltsum, U.; Kurniawan, A.F.; Nurhasanah, I.; Priyono, P. The Role of Concentration Ratio of TTiP:AcAc on the Photocatalytic Activity of TiO<sub>2</sub> Thin Film in Reducing Degradation Products of Used Frying Oil. *Bull. React. Eng. Catal.* **2017**, *12*, 430–436.
29. Siwinska-Stefanska, K.; Zdzarta, J.; Paukszta, D.; Jesionowski, T. The influence of addition of a catalyst and chelating agent on the properties of titanium dioxide synthesized via the sol–gel method. *J. Sol.-Gel Sci. Technol.* **2015**, *75*, 264–278. [[CrossRef](#)]
30. Kajitvichyanukul, P.; Pongpom, S.; Watcharenwong, A.; Ananpattarachai, J. Effect of Acetyl Acetone on Property of TiO<sub>2</sub> Thin Film for Photocatalytic Reduction of Chromium(VI) from Aqueous Solution. *J. Spec. Issue Nanotech.* **2005**, *4*, 87–93.
31. RRUFF – Database. Available online: <http://rruff.info/Anatase/R060277> (accessed on 8 October 2019).
32. Pimpabute, N.; Burinprakhon, T.; Somkunthot, W. Determination of optical constants and thickness of amorphous GaP thin film. *Opt. Appl.* **2011**, *1*.
33. Duminica, F.D.; Maury, F.; Abisset, S. Pyrosol deposition of anatase TiO<sub>2</sub> thin films starting from Ti(OiPr)<sub>4</sub>/acetylacetone solutions. *Thin Solid Films* **2007**, *515*, 7732–7739. [[CrossRef](#)]
34. Stefanov, B.; Österlund, L. Tuning the Photocatalytic Activity of Anatase TiO<sub>2</sub> Thin Films by Modifying the Preferred <001> Grain Orientation with Reactive DC Magnetron Sputtering. *Coatings* **2014**, *4*, 587–601. [[CrossRef](#)]
35. Kumar, K.; Ntwaeaborwa, O.M.; Holsa, J.; Motaung, D.E.; Swart, H.C. The role of oxygen and titanium related defects on the emission of TiO<sub>2</sub>:Tb<sup>3+</sup> nano-phosphor for blue lighting applications. *Opt. Mater.* **2015**, *46*, 510–516. [[CrossRef](#)]
36. Naem, M.; Hasanain, S.K.; Kobayashi, M.; Ishida, Y.; Fujimori, A.; Buzby, S.; Shah, I. Effect of reducing atmosphere on the magnetism of Zn<sub>1-x</sub>CoxO (0 ≤ x ≤ 0.10) nanoparticles. *Nanotechnology* **2006**, *17*, 2675–2680. [[CrossRef](#)] [[PubMed](#)]
37. Gromyko, I.; Krunks, M.; Dedova, T.; Katerski, A.; Klauson, D.; Oja Acik, I. Surface properties of sprayed and electrodeposited ZnO rod layers. *Appl. Surf. Sci.* **2017**, *405*, 521–528. [[CrossRef](#)]

38. Klaysri, R.; Ratova, M.; Praserttham, P.; Kelly, P.J. Deposition of Visible Light-Active C-Doped Titania Films via Magnetron Sputtering Using CO<sub>2</sub> as a Source of Carbon. *Nanomaterials* **2017**, *7*, 113. [[CrossRef](#)] [[PubMed](#)]
39. Zhang, Y.; Zhao, Z.; Chen, J.; Chenga, L.; Changa, J.; Shenga, W.; Huc, C.; Cao, S. C-doped hollow TiO<sub>2</sub> spheres: In situ synthesis, controlled shell thickness, and superior visible-light photocatalytic activity. *Appl. Catal. B-Environ.* **2015**, *165*, 715–722. [[CrossRef](#)]
40. Seo, H.O.; Woo, T.G.; Park, E.J.; Cha, B.J.; Kim, I.H.; Han, S.W.; Kim, Y.D. Enhanced photo-catalytic activity of TiO<sub>2</sub> films by removal of surface carbon impurities; the role of water vapor. *Appl. Surf. Sci.* **2017**, *420*, 808–816. [[CrossRef](#)]
41. Rajkumar, R.; Nisha, S. To Study the Effect of the Concentration of Carbon on Ultraviolet and Visible Light Photo Catalytic Activity and Characterization of Carbon Doped TiO<sub>2</sub>. *J. Nanomed. Nanotechnol.* **2015**, *6*, 7.
42. Shi, Z.J.; Ma, M.G.; Zhu, J.F. Recent Development of Photocatalysts Containing Carbon Species: A Review. *Catalysts* **2019**, *9*, 20. [[CrossRef](#)]
43. Valentin, C.D.; Pacchioni, D.; Selloni, A. Theory of Carbon Doping of Titanium Dioxide. *Chem. Mater.* **2005**, *172*, 66656–66665. [[CrossRef](#)]
44. Banerjee, S.; Dionysiou, D.D.; Pillai, S.C. Self-cleaning applications of TiO<sub>2</sub> by photo-induced hydrophilicity and photocatalysis. *Appl. Catal. B-Environ.* **2015**, *176–177*, 396–428. [[CrossRef](#)]
45. Zheng, J.Y.; Bao, S.H.; Gou, Y.; Jin, P. Natural Hydrophobicity and Reversible Wettability Conversion of Flat Anatase TiO<sub>2</sub> Thin Film. *Appl. Mater. Inter.* **2014**, *6*, 1351–1355. [[CrossRef](#)] [[PubMed](#)]
46. Schneider, J.; Matsuoka, M.; Takeuchi, M.; Zhang, J.; Horiuchi, Y.; Anpo, M.; Bahnemann, D.W. Understanding TiO<sub>2</sub> Photocatalysis: Mechanisms and Materials. *Chem. Rev.* **2014**, *114*, 9919–9986. [[CrossRef](#)] [[PubMed](#)]
47. Sano, T.; Puzenat, E.; Guillard, G.; Geantet, C.; Matsuzawa, S.; Negishi, N. Improvement of Photocatalytic Degradation Activity of Visible-Light-Responsive TiO<sub>2</sub> by Aid of Ultraviolet-Light Pretreatment. *J. Phys. Chem. C* **2009**, *113*, 5535–5540. [[CrossRef](#)]
48. Higashimoto, S.; Katsuura, K.; Yamamoto, M.; Takahashi, M. Photocatalytic activity for decomposition of volatile organic compound on Pt-WO<sub>3</sub> enhanced by simple physical mixing with TiO<sub>2</sub>. *Catal. Commun.* **2020**, *133*, 1566–7367. [[CrossRef](#)]
49. Mills, A.; Lepre, A.; Elliott, N.; Bhopal, S.; Parkin, I.P.; O’Neill, S.A. Characterisation of the photocatalyst Pilkington Activ™: A reference film photocatalyst? *J. Photoch. Photobio. A* **2003**, *160*, 213–224. [[CrossRef](#)]
50. Mills, A.; Wang, J. Simultaneous monitoring of the destruction of stearic acid and generation of carbon dioxide by self-cleaning semiconductor photocatalytic films. *J. Photoch. Photobio. A* **2006**, *182*, 181–186. [[CrossRef](#)]
51. Pore, V.; Ritala, M.; Lekelä, M.; Areva, S.; Järn, M.; Järnström, J. H<sub>2</sub>S modified atomic layer deposition process for photocatalytic TiO<sub>2</sub> thin films. *J. Mater. Chem.* **2007**, *17*, 1361–1371. [[CrossRef](#)]
52. Smirnova, N.; Fesenko, T.; Zhukovsky, M.; Goworek, J.; Eremenko, A. Photodegradation of Stearic Acid Adsorbed on Superhydrophilic TiO<sub>2</sub> Surface: In Situ FTIR and LDI Study. *Nanoscale Res. Lett.* **2015**, *10*, 7. [[CrossRef](#)]
53. Montero, J.; Österlund, L. Photodegradation of Stearic Acid Adsorbed on Copper Oxide Heterojunction Thin Films Prepared by Magnetron Sputtering. *ChemEngineering* **2018**, *2*, 40. [[CrossRef](#)]
54. Wang, S.-H.; Chen, T.-K.; Rao, K.K.; Wong, M.-S. Nanocolumnar titania thin films uniquely incorporated with carbon for visible light photocatalysis. *Appl. Catal. B-Environ.* **2007**, *76*, 328–334. [[CrossRef](#)]
55. Ratova, M.; Klaysri, R.; Praserttham, P.; Kelly, P.J. Visible light active photocatalytic C-doped titanium dioxide films deposited via reactive pulsed DC magnetron co-sputtering: Properties and photocatalytic activity. *Vacuum* **2018**, *149*, 214–224. [[CrossRef](#)]
56. Varnagir, S.; Medvids, A.; Lelis, M.; Milcius, D.; Antuzevics, A. Black carbon-doped TiO<sub>2</sub> films: Synthesis, characterization and photocatalysis. *J. Photochem. Photobio. A-Chem.* **2019**, *382*, 9. [[CrossRef](#)]
57. Aiyong, B.; Wei, L.; Gengle, Z.; Jinbo, X. Preparation and Enhanced Daylight-Induced Photo-Catalytic Activity of Transparent C-Doped TiO<sub>2</sub> Thin Films. *J. Wuhan Univ. Tehnol.-Mater. Sci. Ed.* **2010**, *25*, 738–742.

58. Klauson, D.; Poljakova, A.; Pronina, N.; Krichevskaya, M.; Moiseev, A.; Dedova, T.; Preis, S. Aqueous Photocatalytic Oxidation of Doxycycline. *Adv. Oxid. Technol.* **2013**, *16*, 234–243. [[CrossRef](#)]
59. Klauson, D.; Budarnaja, O.; Stepanova, K.; Krichevskaya, M.; Dedova, T.; Käkinen, A.; Preis, S. Selective Performance of Sol–Gel Synthesised Titanium Dioxide Photocatalysts in Aqueous Oxidation of Various-Type Organic Pollutants. *Kinet. Cata.* **2014**, *55*, 47–55. [[CrossRef](#)]

**Sample Availability:** Samples of the compounds are available from the authors.



© 2019 by the authors. Licensee MDPI, Basel, Switzerland. This article is an open access article distributed under the terms and conditions of the Creative Commons Attribution (CC BY) license (<http://creativecommons.org/licenses/by/4.0/>).